



# iceast 2018

The 4<sup>th</sup> International Conference on Engineering,  
Applied Sciences and Technology

**July 4-7, 2018**

**Swissôtel Resort Phuket Patong Beach  
Phuket, Thailand**

**[www.iceast.org](http://www.iceast.org)**

# Fully Active and Minimal Shadow Bandpass Filter

Seangrawee Buakaew

Department of Electronic Engineering  
Faculty of Engineering,  
King's Mongkut Institute of Technology  
Ladkrabang, Bangkok, Thailand.  
Seangrawee.to@kmitl.ac.th

Wipavan Narksarp

Department of Electrical Engineering  
Faculty of Engineering,  
Siam University, Bangkok, Thailand.  
wipavan.nar@siam.edu

Chariya Wongtaychatham

Department of Electronic Engineering  
Faculty of Engineering,  
King's Mongkut Institute of Technology  
Ladkrabang, Bangkok, Thailand.

**Abstract**—A new topology of shadow bandpass filters is presented in this paper. The proposed circuit employs the active building block of three voltage differencing transconductance amplifiers (VDTA) along with two grounded capacitors. This results in an additional attractive feature of being fully active and minimal component-count. Practical realization of the VDTA is also given and employed for circuit verification. PSPICE simulation with model parameters of 0.18  $\mu\text{m}$  CMOS technology is included to confirm the filter functionality of the proposed filter.

**Keywords**—shadow bandpass filter; VDTA; frequency agile filter.

## I. INTRODUCTION

Since the first introduction of the shadow filters which is also known as frequency agile filters [1,2], the topic has continually drawn attention among researchers. This type of filters offer easy access to modify the characteristic parameters of the filter. That the center frequency rapidly hops over a wide range of frequencies boosts an interest for applications in advance communication systems such as cognitive radio and encrypted communications. Over the past few years, numerous researches to implement the shadow filters have been developed [2-5]. In [2], the shadow filter is realized in current-mode using the current controlled conveyors (CCCII+). The circuit gives electronic tunability of the filter center frequency via the gain of an external amplifier. In [3], the shadow filter with improved bandwidth and quality factor is proposed using a number of active elements for circuit realization. It essentially employs two z-copy current inverter transconductance amplifiers (ZC-CITA) with two variable current amplifiers. In [4], the shadow filter, the active elements of which are current feedback operational amplifiers (CFOAs). The proposed configuration demonstrates the advantage of reduction of the summing node. In [5], another shadow bandpass filter is developed with the use of active building blocks of the so-called differential difference current conveyors (DDCCs). Still quite a large number of external resistors are used. It is noticed that the schemes of [4] and [5] lack electronic tunability feature. The property of electronic tunability in the shadow bandpass filter can be founded in [8] and [9]. They are realized based on the active elements so-called the current differencing transconductance amplifiers (CDTAs). In [8], two CDTAs and in [9] three CDTAs are used along with a number of passive resistors.

In this paper, new configuration of the shadow bandpass filters are presented in voltage-mode. Firstly proposed is the circuit configuration realized by using three voltage differencing transconductance amplifiers (VDTAs) together with only two grounded capacitors and without any external resistors needed. Then the proposed circuit is further extended so as to obtain a more concise circuit configuration. The merits of the two proposed circuits include

a smaller component-count, comparing with the existing work of the same kind so far, which incorporate both active elements as well as passive elements used in the circuit. Also, the filter characteristics, i.e., the center frequency and the quality factor can be electronically adjusted via the bias current of the VDTAs. Moreover, the present work yields a constant bandwidth while tuning the center frequency. In addition, while cling to the concept of being agile bandpass filter, the center frequency and the quality factor are easily controlled via the dc bias current of the VDTAs. Last but not least, the proposed filters do not require any matching constraint on the components used. The aforementioned advantages make the circuits attractive for IC-integration process.

## II. BASIC PRINCIPLE

### A. Concept of the Shadow Bandpass Filter

It is well-known that second-order filter plays a significant role in various fields of analog electronics. Fig. 1 shows a block diagram of the second-order filter with one bandpass and one lowpass outputs, the transfer functions of which are, respectively, as follows

$$H_{BP}(s) = \frac{V_{BP}(s)}{V_{in}(s)} = \frac{K_B s}{1 + as + bs^2} \quad (1)$$

$$H_{LP}(s) = \frac{V_{LP}(s)}{V_{in}(s)} = \frac{K_L}{1 + as + bs^2} \quad (2)$$

The center frequency of the bandpass filter is given by  $f_{01} = \frac{1}{2\pi\sqrt{b}}$

with the gain at this frequency being  $\frac{K_B}{a}$ . The quality factor is given

by  $Q_{01} = \frac{\sqrt{b}}{a}$ . The -3dB bandwidth is  $\Delta f = \frac{a}{2\pi b}$ .

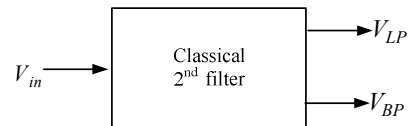


Fig. 1 Block diagram of the classical second order filter

Fig. 2 displays the principle of the shadow bandpass filter [1]. It shows the second-order filter with the lowpass output being fed back through an amplifier of an adjustable gain A. Tuning the gain of the external allows simultaneous changes of the center frequency and the quality factor while the bandwidth is kept constant. Note that this is

possible without disturbing the internal structure of the second-order filter, itself. A few steps of manipulation produce the following transfer function for the bandpass filter

$$T_{BP}(s) = \frac{V_{BP}(s)}{V_{in}(s)} = \frac{\frac{K_B s}{1 + AK_L}}{1 + \frac{as}{1 + AK_L} + \frac{bs^2}{1 + AK_L}} \quad (3)$$

Hence, the shadow bandpass filter in Fig.2 yields the following characteristics

$$f_{02} = \sqrt{1 + AK_L} f_{01} \quad (4)$$

$$Q_{02} = \sqrt{1 + AK_L} Q_{01} \quad (5)$$

Again, the -3dB bandwidth  $\Delta f = \frac{a}{2\pi b}$

It is noted that the -3dB bandwidth of the shadow bandpass filter remains the same as that of Fig. 1.

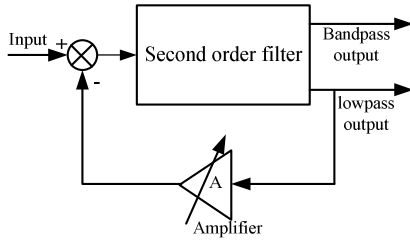


Fig. 2 The basic concept of the shadow bandpass filter

### B. VDTA and Validation Circuit

The VDTA is one popular active building block in designing analog circuitry. Fig. 3 shows the symbol of the VDTA with the description as expressed in (6)

$$\begin{bmatrix} I_Z \\ I_{X+} \\ I_{X-} \end{bmatrix} = \begin{bmatrix} g_{m1} & -g_{m1} & 0 \\ 0 & 0 & g_{m2} \\ 0 & 0 & -g_{m2} \end{bmatrix} \begin{bmatrix} V_{Vp} \\ V_{Vn} \\ V_Z \end{bmatrix} \quad (6)$$

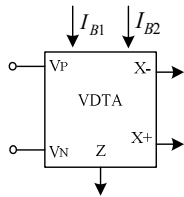


Fig. 3 Circuit symbol of the VDTA

A practical circuit realization of the VDTA [6] employing the CMOS technology is shown in Fig. 4 which is to be used for circuit verification of the present work.

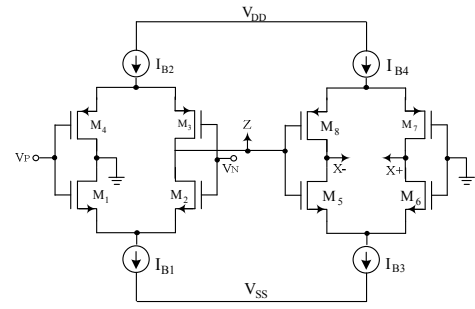


Fig. 4 Practical realization of the VDTA

### III. THE PROPOSED SHADOW BANDPASS FILTERS

Firstly proposed is the shadow bandpass filter employing only three VDTAs and two grounded capacitors. The circuit configuration is shown in Fig. 5. In the figure, VDTA I is the general voltage amplifier with an adjustable gain controlled by the bias currents of the device. The voltage gain can be easily founded as

$$\frac{V_{FB}(s)}{V_{LP}(s)} = A = \frac{g_{m1}}{g_{m2}} \quad (7)$$

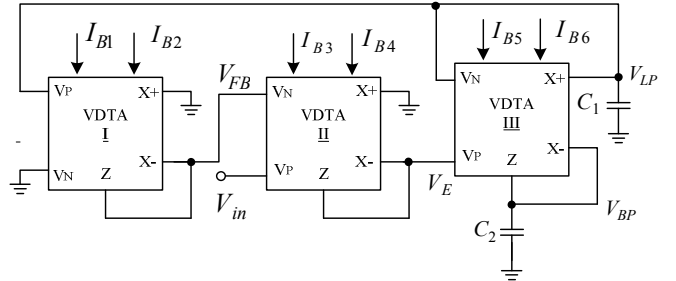


Fig. 5 The proposed shadow bandpass filter

Next, VDTA II is a differential amplifier. The transfer function from the differential inputs to the output is founded as follows

$$\frac{V_E(s)}{V_{in}(s) - V_{FB}(s)} = K = \frac{g_{m3}}{g_{m4}} \quad (8)$$

Using the relationship in (6) for routine analysis results in the following transfer functions for, respectively, the bandpass and lowpass filters

$$\frac{V_{BP}(s)}{V_{in}(s)} = \frac{\frac{KsC_1}{g_{m6}}}{1 + AK + s \frac{C_1}{g_{m5}} + s^2 \frac{C_1 C_2}{g_{m5} g_{m6}}} \quad (9)$$

$$\frac{V_{LP}(s)}{V_{in}(s)} = \frac{K}{1 + AK + s \frac{C_1}{g_{m5}} + s^2 \frac{C_1 C_2}{g_{m5} g_{m6}}} \quad (10)$$

Then the center frequency can be readily extracted from (9)

$$f_0 = \frac{1}{2\pi} \sqrt{(1 + AK) \frac{g_{m5} g_{m6}}{C_1 C_2}} \quad (11)$$

Clearly seen in (11), the shadow bandpass filter possesses the center frequency which is proportional to the term  $\sqrt{1+AK}$ .

Therefore the center frequency can be promptly tuned by controlling the amplifiers' gains. Meanwhile, from (9) the quality factor of the shadow bandpass filter is obtained as

$$Q = \sqrt{(1+AK) \frac{g_{m5}C_2}{g_{m6}C_1}} \quad (12)$$

The bandwidth is corresponding achieved as

$$BW_{-3dB} = \frac{g_{m6}}{2\pi C_2} \quad (13)$$

From (13), it is noticed that the bandwidth can be kept constant while the center frequency is steered around via the amplifiers's gains.

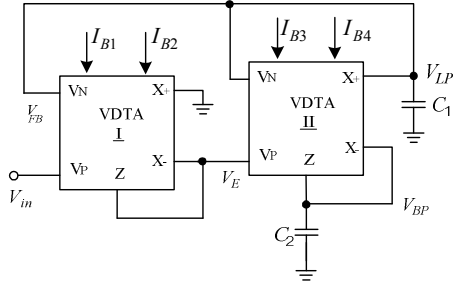


Fig.6 The second proposed shadow filter

Secondly proposed is the shadow bandpass filter which is further modified from the one just having been discussed. Fig. 6 depicts the new configuration of the proposed shadow bandpass filter which consists of only two VDTAs and two grounded capacitors. The circuit analysis is similar to that of Fig. 5. In Fig. 6, VDTA I is an amplifier having the transfer function as follows:

$$\frac{V_E(s)}{V_{in}(s) - V_{FB}(s)} = K = \frac{g_{m1}}{g_{m2}} \quad (14)$$

Using the relationship (6), the circuit in Fig. 6 can be analyzed to yield, respectively, the following bandpass and lowpass transfer functions

$$\frac{V_{BP}(s)}{V_{in}(s)} = \frac{KsC_1}{g_{m4} \left( 1 + K + s \frac{C_1}{g_{m3}} + s^2 \frac{C_1C_2}{g_{m3}g_{m4}} \right)} \quad (15)$$

$$\frac{V_{LP}(s)}{V_{in}(s)} = \frac{K}{g_{m3} \left( 1 + K + s \frac{C_1}{g_{m3}} + s^2 \frac{C_1C_2}{g_{m3}g_{m4}} \right)} \quad (16)$$

Obviously from (15), the center frequency is obtained as

$$f_0 = \frac{1}{2\pi} \sqrt{(1+K) \frac{g_{m3}g_{m4}}{C_1C_2}} \quad (17)$$

Then the corresponding quality factor is founded as

$$Q = \sqrt{(1+K) \frac{g_{m3}C_2}{g_{m4}C_1}} \quad (18)$$

Finally, the -3 dB bandwidth is expressed as follows:

$$BW_{-3dB} = \frac{g_{m4}}{2\pi C_2} \quad (19)$$

#### IV. VERIFICATION RESULTS

The theoretical analysis of the two proposed shadow bandpass filters has been verified with PSPICE simulation. The process parameters rely on the TSMC CMOS 0.18 $\mu$ m. The CMOS topology shown in Fig. 3 is used for practical realization of the VDTA active building block. The CMOS dimensions are given in Table 1. The supply voltages are taken values of  $V_{DD} = -D_{SS} = 1V$ . The transconductance gains are electronically controlled by tuning the bias current  $I_B$  of the VDTAs. First the shadow filter bandpass filter in Fig. 5 is simulated with  $I_{B3} = I_{B4} = 100\mu A$  and hence,  $K=1$ . The second order filter is biased using  $I_{B5} = I_{B6} = 100\mu A$  and  $C_1 = C_2 = 20$  pF. Then variation of the amplifier gain A, through the bias current  $I_{B2}$ , is studied. Let  $I_{B1} = 200\mu A$  while varying  $I_{B2}$  as follows :  $I_{B2} = 40\mu A$  ( $A=5$ ),  $60\mu A$  ( $A=3.34$ ),  $80\mu A$  ( $A=2.5$ ),  $100\mu A$  ( $A=2$ ). The corresponding responses are illustrated in Fig. 7. The responses obviously demonstrate that the center frequency hops from one value to another. Also it is noticed that the bandwidth remains constant as the center frequency steers towards a certain value. The power dissipation of the circuit is about 1.4 mW at the maximum bias point. The signal to noise ratio (SNR) is 27.3 dB at node output.

Table I. CMOS dimension of VDTA

Transistors	W ( $\mu$ m)	L ( $\mu$ m)
M <sub>1</sub> , M <sub>2</sub> , M <sub>5</sub> , M <sub>6</sub>	3.6	0.36
M <sub>3</sub> , M <sub>4</sub> , M <sub>7</sub> , M <sub>8</sub>	16.64	0.36

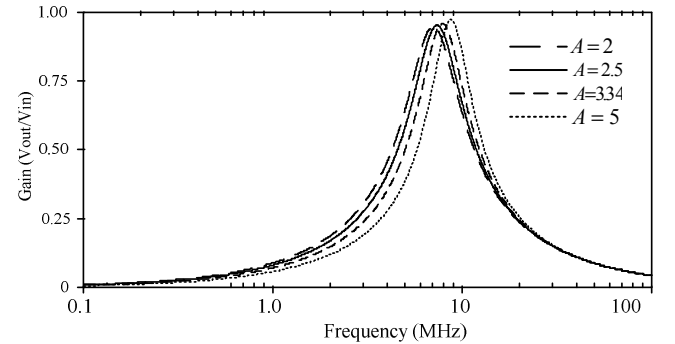


Fig. 7 Frequency responses of the proposed shadow bandpass filter in Fig. 5

The center frequency of the proposed bandpass filter is investigated by using the different gain parameters ( $K=1, 5, 10$ ). At the same time, the gain A are tuned from 2-20 by adjusting the bias current  $I_{B2}$  (constant  $I_{B1} = 200\mu A$ ). The relationship between the center frequency and the gains are presented by graphs in Fig. 8. Clearly, the center frequency swiftly hops to the other frequency. The hopping frequency range depends on the product of gain KA.

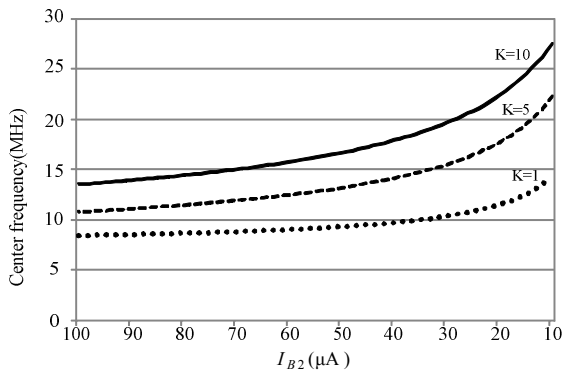


Fig. 8 Relationship of the center frequency and gains

Next the circuit in Fig. 6 is simulated following the same steps as those for Fig. 5. The filter is biased with the dc current equal to  $I_{B3} = I_{B4} = 100 \mu A$  and using  $C_1 = C_2 = 20pF$  for filter parameters. The bias current of the amplifier are  $I_{B2} = 10\mu A$  while  $I_{B1}$  is tuned as  $30 \mu A$  ( $K=3$ ),  $60 \mu A$  ( $K=6$ ) and  $90 \mu A$  ( $K=9$ ) respectively. From the responses, the center frequency is about 8.2MHz, 9.7 MHz and 11.01MHz. It is clear that the propose circuit functions satisfactorily well, in spite of the disappearance of one tuning gain (A).

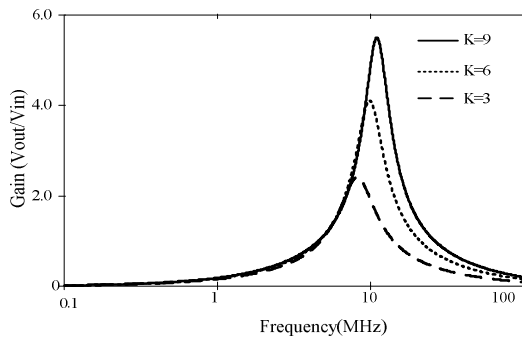


Fig. 8 Frequency responses of the second proposed shadow filter in fig. 6

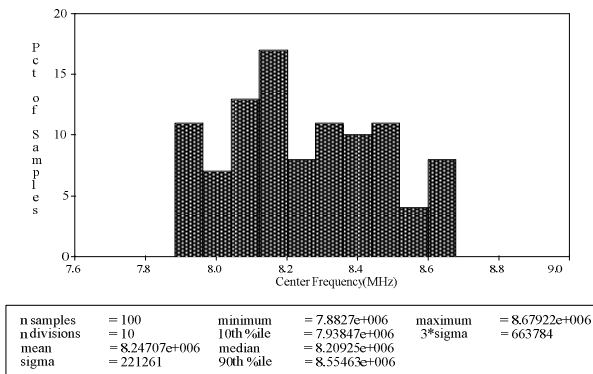


Fig. 9 Monte-Carlo statistical result of BP filter in Fig. 6 with 10% deviation in capacitor values

In addition, the effect of passive component variation on the center frequency response is inspected. A Monte-Carlo statics analysis is the method for evaluation of the proposed filter in Fig. 6. In this simulation, the capacitor value deviates with 10% in normal distribution ( $C_1 = 20pF \pm 10\%$ ) while the number of sample equal to

100 simulation run times and the gain  $K=3$ . The simulation results of a Monte-Carlo statics analysis is shown as histogram in fig. 9. From the result, there are about 68% of center frequency deviated 22.12 kHz from the standard value of center frequency. In addition, the worst case simulations of the all devices are simulated under the same bias conditions. The center frequencies of the worst case in direction high and low are 7.8MHz and 8.6 MHz, respectively (the nominal 8.2MHz). Therefore, the simulation results confirm that the proposed filter works with appropriate sensitivity.

Table II. Feature-comparison of the reported shadow filters with the proposed circuit

Ref.	Number of Component	Number Resistor	Number capacitor	Electronic tuning
[2]	4 CCCII	0	2	Yes
[3]	2 CITA + 2 AMP	0	2	Yes
[4]	4 CFOA	7	2	No
[5]	3/4 DDCC	4/5	2	No
Proposed	2/3 VDTA	0	2	Yes

## V. CONCLUDSION

This paper presents new realization of two shadow bandpass filters based on the active devices VDTAs. The first-presented circuit employs as small number of the VDTAs as only 3. The circuit realization is further improved in terms of reduced component-count. The second circuit is proposed only with the use of only two VDTAs. Passive elements utilized for both configurations are only two grounded capacitors. Hence, the reported circuits are well-suited for monolithic implementation. The validity of the proposed theory is confirmed by simulation. The simulation results exhibit satisfaction for both reported shadow bandpass filter.

## REFERENCES

- [1] Y. Lakys, B. Godara, and A. Fabre, "Cognitive and encrypted communications, part 2: a new approach to active frequency-agile filters and validation results for an agile bandpass topology in SiGe-BiCMOS", in Proceedings of the 6th International Conference on Electrical and Electronics Engineering (ELECO'09), pp.II16-II29, 2009
- [2] Y. Lakys and A. Fabre, "Shadow filters – new family of second-order filters", Electronics Letters, Vol. 46, 2010, pp. 276-277
- [3] V. Biolkova and D. Birolek, "Shadow filters for orthogonal modification of characteristic frequency and bandwidth", Electronics Letters, Vol. 46, 2010, pp. 830-831
- [4] M. T Abuelma'atti, N. Almutairi, "New CFOA-based shadow bandpassFilter", Int. Conf. Electronics, Information, and Communications (ICEIC), 2016, pp. 1–3
- [5] F. Khateb, W. Jaikla, T. Kulej, M. Kumngern, D. Kubánek, "Shadow filter based on DDCC", IET Circuits, Devices & Systems, Vol. 11, 2017, pp. 631-637
- [6] A. Yesil, F. Kacar, H. Kuntman, "New realization of voltage differencing transconductance amplifier and its rf filter application", Radioengineering, Vol. 20, 2011, pp 632-637
- [7] The MOSIS Service, United States. *Wafer electrical test data and SPICE model of TSMC 0.18 μm CMOS process parameter*. 4pages. [Online] Cited 2012-01-31. Available at: <http://www.mosis.org/test/>.
- [8] N.Pandey, R.Pandey, R.Choudhary, A.Sayal and M.Tripathi, "Realization of CDTA based Frequency agile filter". Int. Con. signal processing, computing and control (ISPCC), 2013, pp 1-6
- [9] M. Atasoyu; H. Kuntman; B. Metin; N. Herencsar and O. Cicekoglu, "Design of current mode class 1 frequency agile filter employing CDTAs", European Con. On circuit theory and design (ECCTD), 2015, pp 1-4